C21

Adenosine reverses the development of continuous epileptiform activity in slices from rat entorhinal cortex

Emin Avsar and Ruth M. Empson

School of Biological Sciences, Royal Holloway University of London, Egham, Surrey TW20 OEX, UK

The entorhinal cortex is a highly seizure-prone region of the limbic system. Removal of Mg^{2+} from the perfusate surrounding entorhinal cortex slices generates spontaneous seizure-like events (SLEs) that develop into continuous epileptiform activity resembling status epilepticus (Zhang *et al.* 1995). Here we show that the inhibitory actions of the endogenous neuromodulator adenosine (Dunwiddie, 1999) can reverse the development of this latter type of continuous epileptiform activity.

Horizontal combined hippocampal entorhinal cortex slices (500 μm thick) were prepared from humanely killed female Wistar rats (~200 g). Wedges of the entorhinal cortex (2–3 mm wide) were transferred to a two-compartment chamber that was continuously perfused (2–2.5 ml min^{-1}) with a solution containing (mM): NaCl 135, KCl 3, NaH_2PO_4 1.25, $MgCl_2$ 1, $CaCl_2$ 2, glucose 10 and $NaHCO_3$ 26, pre-equilibrated with 95 % O_2–5 % CO_2 at room temperature. Withdrawal of Mg^{2+} led to the appearance of repetitive SLEs. Drugs were applied via the perfusate and changes in frequency and duration of the SLEs were measured before and after drug application. Values stated are means ± S.E.M.

Adenosine (10 μM) reduced the frequency of SLEs by 28 ± 4 % ($n = 36$, $P < 0.001$, Student's paired t test), whereas the adenosine A_1 receptor antagonist 8-cyclopentyl-1,3-dipropylxanthine (DPCPX; 10 nM) increased the frequency of the events dramatically by 515 ± 79 % ($n = 12$, $P < 0.001$, paired t test) and converted the SLEs to a pattern of continuous epileptiform activity. In approximately 10 % of the slices SLEs spontaneously converted to a similar type of continuous pattern, with a mean change in frequency of 1351 ± 276 % ($n = 13$, $P < 0.001$, paired t test). Adenosine (30 μM), reversed this activity back to SLEs with a clear frequency reduction of 69 ± 3 % ($n = 4$, $P < 0.01$, paired t test). Erythro-9-(2-hydroxy-3-nonyl)adenine (EHNA; 1 μM), an adenosine deaminase inhibitor that increases extracellular adenosine levels, exerted a similar reversal, reducing the frequency of the continuous activity by 63 ± 8 % ($n = 5$, $P < 0.05$, paired t test) whilst DPCPX (0.1 μM) had no significant effect ($n = 5$).

Our results suggest that endogenous adenosine normally released during SLEs prevents the transition to a continuous pattern of epileptiform activity and that spontaneous transitions may be favoured when adenosine levels become depleted.

Dunwiddie TV (1999). *Adv Neurol* **79**, 1001–1010.

Zhang CL *et al.* (1995). *Epilepsy Res* **20**, 105–111.

We acknowledge the support of the Epilepsy Research Foundation, UK.

All procedures accord with current UK legislation.

C23

Hypoxia occludes activation of hTREK1 by intracellular acidosis

P. Miller*, C. Peers† and P.J. Kemp*

*Schools of * Biomedical Sciences and † Medicine, University of Leeds, Leeds LS2 9JT, UK*

The human tandem-P domain K^+ channel, hTREK1, is O_2 sensitive and hypoxia occludes its modulation by arachidonic acid or membrane deformation (Miller *et al.* 2003). These findings question the neuroprotective role of hTREK1 during central ischaemia proposed by Honore *et al.* (2002). Here we report the effects of altered intracellular pH (pH_i) on the ability of hypoxia to inhibit this channel.

All experiments employed whole-cell patch clamp recordings from HEK293 cells stably transfected with hTREK1, and data reported are taken from currents recorded at a step potential of +60 mV from a holding potential of −70 mV (see Miller *et al.* 2003).

Current density measured 20 s following the transition to whole-cell configuration was not dependent upon pH_i. Thus, at pH_i 6.5 (using 11 mM Pipes to buffer pH_i; $n = 6$) current density was 282 ± 115 pA pF^{-1} (mean ± S.E.M.) whilst at pH_i 7.2 (11 mM Hepes; $n = 10$) and pH_i 7.9 (11 mM Tris; $n = 5$), current densities were 173 ± 53 pA pF^{-1} and 157 ± 46 pA pF^{-1}, respectively. Subsequently, mean current density of each cohort steadily increased in a pH_i-dependent manner to 654 ± 198 pA pF^{-1} (pH 6.5), 410 ± 80 pA pF^{-1} (pH 7.2) and 263 ± 46 pA pF^{-1} (pH 7.9) after 2–4 min. Thus, hTREK1 whole-cell current amplitude was sensitive to pH_i. Furthermore, acute hypoxia (~20 mmHg) evoked current depression at all three pH_i values with the hypoxia-sensitive current being largest at low pH_i.

In order to test the hypothesis that pH_i and hypoxia are interacting modulatory influences on this important neuronal channel, we investigated the effect of dynamically altering pH_i using extracellular addition of 20 mM sodium propionate. This evoked rapid and significant (Student's paired t test) channel activation from 228 ± 32 pA pF^{-1} to 299 ± 33 pA pF^{-1} ($P < 0.005$, $n = 9$). In the continued presence of propionate, hypoxia reduced this to 168 ± 18 pA pF^{-1} ($P < 0.0005$). This 42 ± 4 % inhibition was significantly larger than the 26 ± 3 % reduction seen in the absence of weak acid ($n = 13$, $P < 0.002$, Student's unpaired t test). Importantly, the absolute magnitude of the currents in hypoxia alone was not different from that following co-application of weak acid with hypoxia; i.e. acid activation is occluded by hypoxia.

Together with our previous data (Miller *et al.* 2003), these new observations show that many of the stimuli associated with ischaemia/hypoxia (such as arachidonic acid release, cell swelling, and acid insult) cannot activate hTREK1 when O_2 availability is limited and reinforce our earlier suggestion that the proposed neuroprotective role of this channel during ischaemia/hypoxia is unlikely to occur at P_{O_2} values typical in the brain either in health or during pathology.

Honore E *et al.* (2002). *EMBO J* **21**, 2968–2976.

Miller P *et al.* (2003). *J Physiol* **548**, 31–37.

This work was funded by The British Heart Foundation, The Wellcome Trust and GlaxoSmithKline

C24

The acid-sensitive K^+ channel TASK-1: the implications of twofold symmetry for pH dependence and ionic selectivity

K.H. Yuill, I. Ashmole and Peter R. Stanfield

Molecular Physiology Group, Department of Biological Sciences, University of Warwick, Coventry CV4 7AL, UK

We expressed murine TASK-1 in oocytes from *Xenopus* anaesthetised by immersion in 0.3 % w/v MS222 and killed by destruction of the brain and spinal cord. We used two-electrode voltage clamp to investigate pH sensitivity and ionic selectivity. We mutated two residues, H98 in the first pore domain P1 and D204 in P2. We used a tandem dimer construct to mutate residues in one only of two subunits forming the ion channel. We fitted the pH sensitivity of wild-type TASK-1 assuming that only one His residue (H98) need be protonated for channels to be non-conducting (Ashmole *et al.* 2001).

The experimental results may be fitted using an equilibrium constant, K_a, for the protonation reaction of 9.55×10^{-7} M ($pK_a = 6.02$) at +40 mV (70 mM $[K^+]_o$). The effect was weakly voltage dependent. The requirement for only a single His to be protonated is supported by the finding that pH dependence is conserved in tandem dimers with a single H98D mutation. However pK_a was raised to 7.04 at +40 mV. This change is presumably caused by the introduction of a further acidic residue close to H98. The mutation H98D itself (i.e. in both subunits) reduces, but does not abolish, pH dependence, indicating that residues other than H98 contribute. Surprisingly, the mutation D204H forms channels whose activity is virtually independent of pH over the physiological range. While protonation of H98 appears to be necessary for channel closure, it may not be sufficient. Like Lopes *et al.* (2001), we believe that the response to acidification is not simply through channel blockage, but involves a gating process.

Mutation of H98 and of D204 also alters channel selectivity measured from the shift in reversal potential when 70 mM K^+ is replaced by Rb^+ or Na^+. P_{Rb}/P_K was 0.80 ± 0.03 ($n = 14$; mean ± S.E.M.) in wild-type, 0.84 ± 0.04 ($n = 19$) in H98D and 1.06 ± 0.04 ($n = 19$) in D204H. At negative voltages, Rb^+ currents were smaller than K^+ currents in wild-type, but were larger in D204H. Channels became substantially Na^+ permeable after mutation. In wild-type, P_{Na}/P_K was less than 0.09. But it was 0.39 ± 0.03 ($n = 14$) in H98D and 0.64 ± 0.04 ($n = 18$) in D204H. In D204H, Na^+ currents were approximately 30 % the amplitude of K^+ currents at negative voltages; at positive voltages, Na^+ in the external solution blocked the efflux of K^+. We find that twofold symmetry best supports both pH sensitivity over the physiological range and K^+ selectivity.

Ashmole I *et al.* (2001). *Pflugers Arch* **442**, 828–833.

Lopes CMB *et al.* (2001). *J Biol Chem* **276**, 24449–24452.

We thank the BBSRC for support

All procedures accord with current UK legislation.

C25

Inhibition of γ-secretase reverses an hypoxia-induced increase in K^+ channel currents in rat cerebellar granule neurons

D.B. Freir, N.J. Webster*, L.D. Plant, J.P. Boyle *, M. Ramsden, C. Peers* and H.A. Pearson

*School of Biomedical Sciences and *Institute of Cardiovascular Research, University of Leeds LS2 9JT, UK*

Studies have shown an increased incidence of Alzheimer's disease (AD) in individuals who have suffered an episode of cerebral ischaemia (Moroney *et al.* 1996). The AD related peptide amyloid β protein (Aβ) disrupts cellular ion homeostasis and is increased following hypoxia in PC12 cells (Taylor *et al.* 1999). In addition, we have reported an increase in potassium channel currents in cerebellar granule neurons following application of Aβ (Ramsden *et al.* 2001). Here, we investigated the effects of chronic hypoxia on potassium channel currents in primary cultures of cerebellar granule neurones and examined the potential involvement of Aβ in these effects.

The whole-cell configuration of the patch-clamp technique was used to measure K^+ channel currents. Cells held at −70 mV were prepulsed for 200 ms to −140 or −50 mV before stepping to test potentials between −60 and +70 mV. Untreated cells in addition to those cells treated with the gamma-secretase inhibitor, γ-IV, were incubated in a humidified atmosphere in either normoxic (21 % O_2) or hypoxic (2.5 % O_2) air, at 37 °C for 24–48h. All current values were normalised to whole-cell capacitance and data presented as means ± S.E.M. Western blotting and immunohistochemical staining for Aβ and Kv subunits used the monoclonal antibody 3D6 and polyclonal antibodies, respectively. Statistical comparisons were made using Student's unpaired *t* test.

Chronic hypoxia caused a significant increase in K^+ channel current density when compared to controls. At the +50 mV test potential peak K^+ channel current was 766 ± 50 pA pF^{-1} in normoxic cells ($n = 34$) compared to 961 ± 69 pA pF^{-1} in hypoxia treated cells ($n = 36$), following a prepulse to −140 mV ($P < 0.05$). The gamma secretase inhibitor, γ-IV (3 μM), had no effect on K^+ current under normoxic conditions (797 ± 94 pA pF^{-1}, $n = 25$); however, it caused a reversal of the hypoxia-induced increase in potassium current (860 ± 121 pA pF^{-1}, $n = 24$). Immunofluorescence imaging revealed an increase in Aβ production following chronic hypoxia when compared to normoxic controls. This increase in Aβ was prevented following application of γ-IV. Western blot and immunofluorescence imaging of Kv4.2 and 4.3 suggested that changes in I_{KA} were due to an increase in Kv expression.

These data suggest that the hypoxia-induced increase in K^+ currents in cultured cerebellar granule neurons is, at least in part, due to the increased production of Aβ following chronic hypoxia.

Moroney JT *et al.* (1996). *Stroke* **27**, 1283–1289.

Ramsden M *et al.* (2001). *J Neurochem* **79**, 699–712.

Taylor SC *et al.* (1999). *J Biol Chem* **274**, 31217–31223.

All procedures accord with current UK legislation.

C26

The role of c-Jun N-terminal kinase in lipopolysaccharide-induced cell deterioration in rat hippocampus

Claire E. Barry and Marina A. Lynch

Department of Physiology, Trinity College, Dublin 2, Ireland

Lipopolysaccharide (LPS), a component of the cell wall of Gram-negative bacteria, exerts manifold effects in the central nervous system. It has been reported that I.P. injection of LPS (100 μg kg^{-1}) inhibits LTP in dentate gyrus. While the mechanism by which this is effected remains unclear, LPS administration is associated with activation of stress-activated protein kinases such as c-Jun N-terminal protein kinase (JNK). There is evidence linking these protein kinases to cell deterioration, possibly accounting for the LPS-induced decrease in synaptic efficacy. Here we report that I.C.V. administration of the specific JNK inhibitor D-JNKI1 (5 μl; 500 μM) attenuated the LPS-induced inhibition of LTP of perforant path–dentate gyrus granule cell synapses in urethane-anaesthetised rats.

Following electrophysiological recording, rats were humanely killed by decapitation, and the hippocampus was dissected and frozen until examined. LPS induced an increase in phosphorylated JNK expression in hippocampal tissue (1767 arbitrary units (± 88; S.E.M.) compared to 1448 (± 41) in saline-treated rats ($P < 0.05$; Student's unpaired t test; $n = 5$). Table 1 shows that this activation of JNK by LPS triggers downstream signalling cascades, including activation of the transcription factor c-Jun and Bcl-2 phosphorylation. These changes are coupled with increased cytosolic cytochrome c expression, and Tdt-mediated dUTP nick-end labelling (TUNEL) in cytospun cells, indicative of apoptosis. Pre-treatment with D-JNKI1 attenuated these changes.

Parameter measured (units)	Control Saline	Control LPS	D-JNKI1 Saline	D-JNKI1 LPS
Phosphorylated c-Jun (AU; WB)	1492 (±63)	2127* (±206)	1721 (±161)	1728 (±198)
Phosphorylated bcl-2 (AU; WB)	1730 (±123)	2212* (±176)	1399† (±128)	1681† (±135)
Cytochrome *c* in cytosol (AU; WB)	1559 (±63)	2057* (±192)	1554† (±105)	1930 (±158)
TUNEL stained cells (%; IHC)	7.76 (±1.7)	13.7* (±1.0)	8.32† (±0.8)	9.70† (±1.4)
LTP 40-45min (% epsp slope)	116.0 (±1.4)	97.4* (±0.6)	110.3† (±0.3)	112.4† (±0.8)

* $P < 0.05$; ANOVA; $n > 6$; cf Control Saline.
† $P < 0.05$; ANOVA; $n = 6$; cf Control LPS
AU = Arbitrary Units.
WB= Western immunoblotting, IHC= Immunohistochemistry

Table 1. D-JNKI1 attenuated central effects of LPS. Values are means ± S.E.M.

In summary, the evidence is consistent with a pivotal role for JNK in mediating the effects of LPS.

This work was supported by grants from the Health Research Board (Grant no. RP12/2001), and Enterprise Ireland (Project code BR/2001/009).

All procedures accord with current National and local guidelines.

C27

Imaging activity of individual N-type calcium channels expressed in *Xenopus* oocytes by total internal reflection microscopy

Angelo Demuro and Ian Parker

Department of Neurobiology and Behavior, University of California, Irvine, CA 92697, USA

Patch-clamp recording (Neher & Sakmann, 1976) has revolutionized our ability to study the function of ion channels, but suffers some limitations: notably, it offers little spatial information and cannot provide independent readout from multiple channels. Optical techniques hold promise as a complementary approach, and fluorescence imaging has resolved calcium flux through individual channels (Zou *et al.* 1999; Wang *et al.* 2001; Demuro & Parker, 2002). Further improvements should be possible by localizing calcium signals more tightly around the channel mouth, where changes in calcium concentration are greatest and most rapid. For this purpose total internal reflection fluorescence microscopy (TIRFM) (Axelrod, 2003) is ideal, because the evanescent wave formed by TIR at a glass–water interface extends only a few hundred nanometres. To explore this idea, we imaged calcium flux through N-type channels expressed in *Xenopus* oocytes.

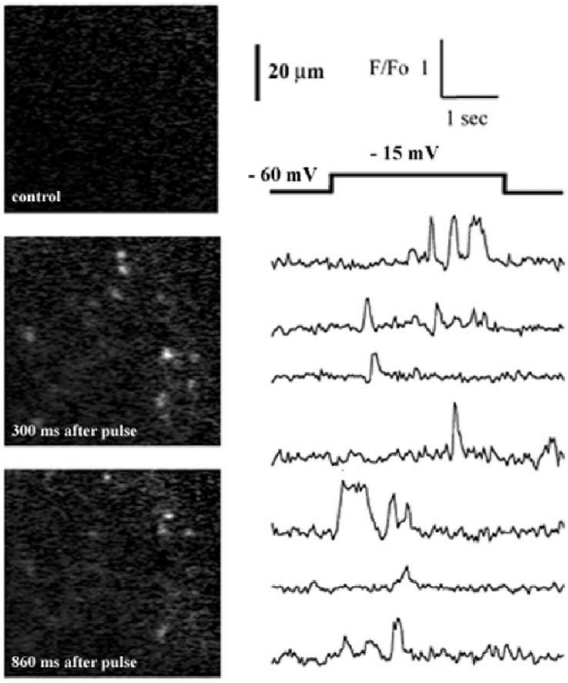

Figure 1. Video frames show fluo-4 fluorescence imaged by TIRFM from a region of oocyte membrane expressing N-type calcium channels when clamped at −60 mV, and at times indicated following depolarization to −15 mV. Traces illustrate local measurements of fluorescence ratio (F/F_0) at several active sites. Data are representative of results in > 50 oocytes (> 1000 channels).

Oocytes were injected with cRNAs for the $\alpha_{1B\text{-}d}$ and β_3 subunits of N-type calcium channels (a kind gift of Dr Dianne Lipscombe). After 4–6 days oocytes were injected with fluo-4 dextran (40 μM final concentration), the vitelline envelope was manually stripped, and oocytes were placed in a chamber constructed from a fresh coverglass and O ring and bathed in Ringer solution including 6 mM calcium. We imaged through an Olympus × 60 NA 1.45 TIRFM objective in an inverted

microscope equipped with an argon ion laser and intensified CCD camera. Depolarizing pulses (applied via a two-electrode voltage clamp) evoked random, pulsatile fluorescence signals (Fig. 1) from many local regions of the cytosol. These are likely to reflect calcium flux through individual channels, because they displayed stochastic kinetics, were absent in non-mRNA-injected oocytes, increased in frequency with a voltage dependence mirroring the gating of N-type channels, and were blocked by 2 μM nickel. Simultaneous measurements could be obtained from >100 channels, with a spatial resolution of < 1 μm and a kinetic resolution (30 ms) at present limited by our video-rate camera.

We anticipate that TIRFM imaging will find wide applications in neuroscience research and high-throughput screening for measurement of functional kinetics and spatial localization of calcium-permeable channels.

Axelrod D (2003). *Meth Enzymol* **361**, 1–33.
Demuro A & Parker I (2002). *Soc Neurosci Abs* 312.2.
Neher E & Sakmann B (1976). *Nature* **260**, 799–802.
Wang SQ *et al.* (2001). *Nature* **410**, 592–596.
Zou H *et al.* (1999). *J Physiol* **492**, 31–38.

This work was supported by NIH grant GM48071

All procedures accord with current National and local guidelines.

C28

Distinct and common properties of N-type and P/Q-type calcium currents at the calyx of Held presynaptic terminal

Taro Ishikawa*, Hee-Sup Shin† and Tomoyuki Takahashi*

**Department of Neurophysiology, University of Tokyo Graduate School of Medicine, Tokyo, Japan and †National CRI Center for Calcium & Learning and Department of Life Science, Pohang University of Science & Technology, Pohang, Republic of Korea*

Nerve-evoked transmitter release at the fast synapse is triggered mainly by N-type and P/Q-type calcium channels. During postnatal development, however, the contribution of N-type calcium channels to synaptic transmission is lost and replaced by P/Q-type calcium currents at many synapses including the calyx of Held (Iwasaki *et al.* 2000).

To address the functional outcome of this developmental switch, using α_{1A} subunit-ablated homozygous mutant and their wild-type littermate (WT) mice (9–12 days old, humanely killed by decapitation under halothane anaesthesia), we compared N-type and P/Q-type presynaptic calcium currents (I_{pCa}) both directly recorded from the calyx of Held nerve terminal visually identified in thin brainstem slices.

I_{pCa} in mutant mice were attenuated by 86% ($n = 4$) by ω-conotoxin GVIA, whereas I_{pCa} in WT mice were attenuated by 87% ($n = 6$) by ω-agatoxin IVA, suggesting that the main component of I_{pCa} in WT and mutant mice is P/Q-type and N-type, respectively. In the current–voltage relationship, I_{pCa} in mutant mice had a peak 5 mV more positive than that of WT mice. In neither mutant nor WT mice did I_{pCa} show a steady-state inactivation (between −130 mV and −40 mV). Inactivation, however, was observed in association with activation in both mutant and WT mice. I_{pCa} undergoes facilitation upon repetitive activation in 8- to 17-day-old rats (Cuttle *et al.* 1998), being mediated by neuronal calcium sensor-1 (Tsujimoto *et al.* 2002). This facilitation was clearly seen in I_{pCa} in WT mice. However, I_{pCa} in mutant mice showed no facilitation in either the paired-pulse or high frequency (100 Hz, 10s) protocols.

We conclude that the activity-dependent I_{pCa} facilitation is a distinct function of P/Q-type calcium channels.

Cuttle MF *et al.* (1998). *J Physiol* **512**, 723–729.
Iwasaki S *et al.* (2000). *J Neurosci* **20**, 59–65.
Tsujimoto T *et al.* (2002). *Science* **295**, 2276–2279.

This work was supported by Grant-in-Aid for Specially Promoted Research from the Ministry of Education, Culture, Sports, Science and Technology.

All procedures accord with current local guidelines.

C29

Characteristics of NMDA responses in hippocampal interneurones and pyramidal cells

E. Avignone, B. Frenguelli and A.J. Irving

Department of Pharmacology and Neuroscience, University of Dundee, Scotland DD1 9SY, UK

Hippocampal interneurons and pyramidal cells differ in their sensitivity to ischaemia and excitotoxic neurodegeneration, with interneurones being markedly less sensitive to these insults (Lipton, 1999). This may reflect differences in Ca^{2+} handling or receptor expression/subunit composition between these cell types. To investigate whether differences in NMDA receptor function could be involved in this phenomenon, we compared electrophysiological and Ca^{2+} responses to NMDA application in pyramidal cells and interneurones in the CA1 hippocampal region.

Hippocampal slices were obtained from 14- to 19-day-old rats, killed humanely by cervical dislocation. Whole-cell patch clamp recording, using a potassium gluconate-based intracellular solution, was combined with ratiometric Ca^{2+} imaging by including the Ca^{2+}-sensitive dye *bis*-fura 2 (150 μM) in the pipette solution. Somatic Ca^{2+} measurements were made using a conventional imaging system (Universal Imaging), with changes in intracellular Ca^{2+} levels expressed as changes in fluorescence ratio units (r.u.). Cell types were identified by their location (pyramidal layer or stratum oriens) and electrophysiological properties. Responses to bath application of NMDA (3–5 min, 10 μM; in the presence of 0.5 μM TTX) were investigated at −60 and −30 mV in both interneurones and pyramidal cells. Data are expressed as means ± S.E.M. and one-way ANOVA was used as the statistical test.

NMDA responses across pyramidal cells were similar and exhibited strong voltage dependence both in the evoked inward current and calcium rise. In pyramidal neurons at −60 mV NMDA induced an inward current of 94.0 ± 18.2 pA ($n = 5$), with a range of 68 to 160 pA. However, this current was associated with no detectable increase in somatic Ca^{2+} levels. When NMDA was applied at −30 mV, it induced a current of 859.0 ± 92.7 pA (7.7 ± 1.1-fold increase) associated with a mean Ca^{2+} rise of 0.77 ± 0.06 r.u. In contrast to pyramidal cells, NMDA responses in interneurones were more heterogeneous, with the inward current varying from 19 to 520 pA at −60 mV (mean 120 ± 55 pA; $n = 9$) and in two cells NMDA application was associated with a small Ca^{2+} rise of 0.05 and 0.17 r.u. The NMDA responses at −30 mV were significantly smaller compared to pyramidal cells ($P < 0.01$). The mean inward current was 254.8 ± 116.6 pA (2.1 ± 0.6-fold increase), associated with a mean Ca^{2+} rise of 0.29 ± 0.1 r.u.

These data show that interneurones and pyramidal cells respond differently to NMDA application with distinct voltage dependence, resulting in enhanced NMDA-evoked Ca^{2+} signals

in pyramidal cells. Such properties could underlie their differing sensitivity to toxic insults.

Lipton P (1999). *Physiol Rev* **79**, 1431–1568.

This work was supported by the BBSRC and EU (Marie Curie).

All procedures accord with current UK legislation.

C30

Physiological differences in somatic and dendritic inhibition in dentate gyrus

S.C. Harney* and Mathew V. Jones†

**Department of Physiology, Trinity College, Dublin 2, Ireland and* †*Department of Physiology, University of Wisconsin–Madison, Madison, Wisconsin 53706, USA*

GABAergic inhibition is mediated by a diverse range of interneuron populations, with distinct anatomical, physiological and biochemical properties which are likely to correlate with specific network functions. We compared the properties of synaptic inhibition at somatic/proximal dendritic synapses formed by fast-spiking (FS) basket cells, with transmission at dendritic synapses formed by non-fast-spiking (NFS), hilar commisural-associational path-related (HICAP) cells on granule cells of the dentate gyrus. In additional experiments we used a dynamic current clamp circuit to inject naturalistic synaptic conductances into interneurons and thus compare their responses to simulated population activity.

Transverse hippocampal slices were prepared from 12- to 20-day-old rats, humanely killed in accordance with the Institutional Animal Care and Use Committee. Dual whole-cell patch clamp recordings were made from interneurons, current-clamped at −60 mV, and granule cells, voltage-clamped at −60 mV. Patch pipettes were filled with 0.1 % biocytin and all interneurons were subsequently identified anatomically. Data are means ± S.E.M. Statistical significance was evaluated using Student's unpaired *t* test ($P < 0.05$).

FS and NFS interneurons had similar resting potentials (−58 ± 1 and −55 ± 1 mV, $n = 27$ FS and 34 NFS) but significantly different input resistances (105 ± 6 *vs.* 202 ± 16 MΩ, $P < 0.05$) and membrane time constants (33 ± 3 *vs.* 49 ± 2 ms, $P < 0.05$). In response to depolarising current steps (1 nA, 1 s) FS cells fired more spikes than NFS cells (72 ± 5 *vs.* 14 ± 3, $P < 0.05$) with a greater maximum spike rate (81 ± 4 *vs.* 65 ± 4 Hz, $P < 0.05$). Granule cell IPSCs evoked by both interneuron populations had similar amplitudes (99 ± 21 pA for FS, $n = 27$, 70 ± 15 pA for NFS, $n = 34$) and decay kinetics ($\tau = 22 \pm 0.8$ ms for FS, 24 ± 1 ms for NFS); however, dendritic NFS IPSCs had slower rise times and synaptic latencies. Paired-pulse depression was greater for NFS (21 ± 0.03 %) than FS IPSCs (16 ± 0.02 %, $P < 0.05$) and IPSCs evoked at 10 and 50 Hz were reliable but strongly depressing for FS synapses, whereas NFS IPSC trains did not show depression. Injection of simulated synaptic conductances, based on synaptic events recorded experimentally, revealed that FS interneurons fired at lower frequencies and with greater precision than NFS cells.

These data indicate that presynaptic physiological properties distinguish somatic and dendritic inhibition and suggest that FS and NFS cells respond differently during network activity.

This work was supported by The Epilepsy Foundation.

All procedures accord with current National and local guidelines.

C31

A role for the PI3K–Akt pathway in long-term potentiation in the dentate gyrus of the rat

Áine Kelly and Marina A. Lynch

Trinity College Institute of Neuroscience, Department of Physiology, Trinity College, Dublin 2, Ireland

Previous studies from our laboratory have suggested a role for nerve growth factor (NGF), and its receptor, TrkA, in long-term potentiation (LTP) in the rat dentate gyrus (Kelly *et al.* 1998, 2000). It therefore seems likely that intracellular signalling pathways activated downstream of the Trk receptor may play a role in the expression of LTP. This study was designed to investigate a possible role for one such pathway, the PI3K–Akt pathway, in LTP. PI3K is an enzyme involved in phospholipid signalling which has been shown to modulate calcium concentration, glutamate release and LTP (Kelly & Lynch 2000) and it is known in several cell types to activate Akt. Both enzymes have recently been suggested to play a role in synaptic plasticity and fear conditioning in the rat amygdala (Lin *et al.* 2001).

In this study we have used the PI3K inhibitor LY294002 to investigate the role of this kinase and its substrate, Akt, in LTP. Male Wistar rats (250–300 g) were anaesthetized with urethane (1.5 g kg^{-1} I.P.). LTP was induced unilaterally in dentate gyrus by tetanic stimulation (3 trains of stimuli of 250 Hz in 50 ms; 30 s inter-train interval) of the perforant path. Test shocks (1/30 s) were delivered to the perforant path for 15 min preceding and 45 min following tetanic stimulation. Intracerebroventricular injection of LY294002 (10 μl; 60 μg ml^{-1} in dimethylsulphoxide; 1 % v/v) 30 min before high-frequency stimulation (HFS) blocked LTP. The mean percentage change in EPSP slope in the last 5 min of the experiment compared with the mean EPSP slope in the 5 min immediately prior to tetanic stimulation was 100.93 ± 4.2 % ($n = 7$; data expressed as means ± S.E.M.) compared with vehicle-injected controls (116.75 ± 1.244 %, $n = 6$). At the end of the recording period, rats were humanely killed by decapitation and untetanized and tetanized dentate gyrii were dissected free, homogenized and stored at −20 °C for analysis. Western immunoblotting using phosphospecific antibodies revealed an increased activation of PI3K and Akt in tetanized compared with untetanized dentate gyrus of control rats; these increases were blocked by prior treatment with LY294002. LY294002 also blocked an LTP-associated activation of mitogen-activated protein kinase (MAPK), suggesting that PI3K may be acting upstream of MAPK.

The data demonstrate that LTP in the rat dentate gyrus is associated with increased activation of PI3K, Akt and MAPK and suggest that inhibition of LTP by LY294002 is a consequence of blockade of activation of these protein kinases.

Kelly Á *et al.* (1998). *Neuropharmacol* **37**, 561–570.
Kelly Á *et al.* (2000). *Neurosci* **95**, 359–365.
Kelly Á & Lynch MA (2000). *Neuropharmacol* **39**, 643–651.
Lin CH *et al.* (2001). *Neuron* **31**, 841–851.

This work was supported by Health Research Board, Ireland.

All procedures accord with current local guidelines.

C32

Inhibitory effect of amyloid-β peptide with the Arctic mutation on long-term potentiation in area CA1 of rat hippocampus *in vivo*

I. Klyubin*, D.M. Walsh†, R. Anwyl‡, D.J. Selkoe† and M.J. Rowan*

** Department of Pharmacology and Therapeutics and ‡Department of Physiology, Trinity College Dublin, Ireland and †Harvard Medical School and Brigham and Women's Hospital, Boston, MA, USA*

The Arctic (E22G) point mutation within the hydrophobic core of amyloid β (Aβ) peptide sequence is associated with a familial form of Alzheimer's disease. The G22 mutation appears to change aggregation of the peptide in the absence of an increase in total Aβ secretion. Previously, we showed that oligomers are the species responsible for the block of long-term potentiation (LTP) by Aβ (Walsh *et al.* 2002). Here we compared the effects of I.C.V. injection of wild-type (WT) and E22G Aβ1–40 peptides on LTP in the CA1 area of urethane (1.5 g kg^{-1} I.P.)-anaesthetised male adult Wistar rats.

The animal care and experimental protocol including humane killing were licensed by the Department of Health, Republic of Ireland. Statistical comparisons were made by Student's paired *t* test. Values are expressed as the mean percentage of the baseline field EPSP amplitude ± S.E.M.

In control, vehicle-injected animals, 200 Hz high frequency stimulation (HFS) induced a robust and stable LTP (148 ± 6 % at 3 h post HFS, $P < 0.0001$, $n = 6$). Aβ WT (5 μl of a 100 μM solution) only partially blocked LTP (122 ± 4 %, $P < 0.001$, $n = 5$) and did not affect baseline synaptic transmission (103 ± 5 % at 3 h post injection, $P > 0.7$, $n = 4$). In contrast, E22G Aβ at a concentration as low as 0.9 μM completely blocked LTP (99 ± 5 %, $P > 0.2$, $n = 4$). Although this concentration of E22G Aβ did not affect baseline transmission (101 ± 4 %, $P > 0.1$, $n = 4$), a higher concentration (42 μM) reduced the baseline EPSP amplitude (62 ± 7 %, $P < 0.005$, $n = 4$). In order to determine if the different activity of the peptides was due to differences in assembly state we performed biophysical characterization of the peptides in solution. The Congo Red assay and electron microscopy showed that while both WT and mutant Aβ formed aggregates, the E22G solution contained larger structures. To compare the relative activities of the peptide in a defined assembly state we removed large aggregates (fibrils) by ultracentrifugation. Injection of this E22G solution (1 μM) also blocked LTP (99 ± 5 %, $P > 0.4$, $n = 6$).

These data suggest that the functional differences between the WT and E22G Aβ peptides may be the result of increased formation of soluble assemblies by the Arctic mutation.

Walsh DM *et al.* (2002). *Nature* **416**, 535–539.

This work was supported by Science Foundation Ireland and the Irish Research Council for Science, Engineering and Technology (M.J.R. and R.A.) and NIH grant (D.J.S.).

All procedures accord with current National guidelines.

C33

Using the t286 CaMKII mutant mouse to probe the locus of cortical plasticity

Neil Hardingham and Kevin Fox

School of Biosciences, Cardiff University, Museum Avenue, Cardiff CF10 3US, UK

The t286 point mutant mouse (T286A) lacks the autophosphorylation site on calcium/calmodulin-dependent protein kinase II (CaMKII). Experiments performed on T286A null mutants prevent experience-dependent plasticity *in vivo* and long term potentiation (LTP) *in vitro* (Hardingham *et al.* 2003). In this study, we aimed to discover whether CaMKII autophosphorylation is required for pre- or postsynaptic changes in synaptic efficacy or indeed both.

Coronal cortical slices were prepared from 4- to 6-week-old wild-type and T286A mice (humanely killed by cervical dislocation). Layer 2/3 neurones in barrel cortex were recorded in current-clamp and stimulated extracellularly in layer 4 of an adjacent barrel. Stimulation was set to a minimal level where single inputs are believed to be activated. Under these circumstances, $1/CV^2$ plots can be used to probe the locus of any change in mean amplitude (Faber & Korn, 1991). Conditioning was achieved by pairing 200 post-synaptic action potentials with presynaptic stimulations at an interval of pre 10 ms before post and at 2 Hz.

In T286A mice, increases in mean amplitude were transient and consistently produced $1/CV^2$ plots consistent with predominantly presynaptic changes ($n = 11$). In wild-types, increases in mean amplitude were stable and produced $1/CV^2$ plots consistent with predominantly postsynaptic changes ($n = 12$). $1/CV^2$ plots were statistically different between T286A and wild-type mice (two sample *t* test, $P < 0.05$). On occasions amplitude frequency histograms had statistically reliable peaks both in control periods of recording and after pairing, possibly referring to the quantal size of excitation. At 5–10 min post-pairing in the control animals, the average distance between peaks often increased ($n = 9$), whereas they remained the same in T286A null mutants ($n = 6$).

Further experiments using APV (50 μM) in the perfusing solution blocked LTP, but produced short-term potentiation (STP) consistent with that seen in T286A mice ($n = 10$). APV had no effect on the STP seen in the T286A mice ($n = 10$) whilst pharmacological blockade of CaMKII with AIP (autocamtide-2-related inhibitory peptide) also blocked potentiation ($n = 5$). Data also suggest long term depression (LTD) is unaffected in the T286A mutants ($n = 11$).

The conclusions of this study are that STP is presynaptic and does not depend on CaMKII autophosphorylation, while LTP also involves a postsynaptic component and is dependent on CaMKII autophosphorylation. LTD is also independent of CaMKII autophosphorylation and can be either pre- or postsynaptic.

Faber DS & Korn H (1991). *Biophys J* **60**, 1288–1294.

Hardingham NR *et al.* (2003). *J Neurosci* **23**, 4428–4436.

All procedures accord with current UK legislation.

C34

Treatment with leupeptin, a calpain inhibitor, improves muscle function following nerve injury in neonatal rats

Dairin Kieran and Linda Greensmith

The Graham Watts Laboratory, Sobell Department of Motor Neuroscience and Movement Disorders, Institute of Neurology, Queen Square, London WC1N 3BG, UK

Developing motoneurons depend on target contact for survival. Injury to the sciatic nerve in neonatal rats leads to extensive motoneuron death resulting in permanent loss of muscle function (Lowrie *et al.* 1987). Injury-induced motoneuron death occurs via a combination of apoptosis and necrosis (Li *et al.* 1998). These processes are mediated by a family of cystine proteases known as calpains (Wang 2000). In this study we examined the effect of treatment with leupeptin, a calpain inhibitor, on the survival and function of motoneurons following neonatal nerve injury.

In 3-day-old rat pups, the sciatic nerve was crushed under halothane anaesthesia (5% halothane in 1.5 l of O_2 per minute) and sterile conditions and a silicon implant containing leupeptin (140 μg mg^{-1}) was applied directly to the spinal cord. Twelve weeks after injury, animals were anaestheisised and prepared for in-vivo assessment of hindlimb muscle function. The distal tendons of both soleus and extensor digitorium longus (EDL) muscles were attached to force transducers and the sciatic nerve was exposed for stimulation. Following assessment all animals were humanely killed. Data are presented as means ± S.E.M. and results were compared statistically using a Mann-Whitney test ($P < 0.05$).

Neonatal nerve injury is known to result in a loss of motor units and a reduction in force of both soleus and EDL muscles. However, in those animals treated with leupeptin, the reduction in muscle function following nerve injury was significantly reduced. Both soleus and EDL have more motor units, are stronger and the change in muscle phenotype induced by nerve injury is prevented. Thus, the maximum tetanic tension (MTT) of the leupeptin-treated soleus muscle was 71.7 ± 10.1 % ($n = 5$) of control compared to only 39.2 ± 7.1 % ($n = 5$) of control in the untreated group. In EDL the MTT of leupeptin-treated animals was 55.6 ± 10.6 % ($n = 5$) of control compared to 34.1 ± 2.1 % ($n = 5$) in the untreated group. Leupeptin treatment also significantly improved motor unit survival so that 12 weeks after injury 20.8 ± 1.40 ($n = 5$) motor units survive compared to only 14.6 ± 1.21 ($n = 5$) in the untreated group. Furthermore, the transformation of muscle fibre phenotype that occurs in EDL muscles following nerve injury was prevented by treatment with leupeptin. Following nerve crush at 3 days EDL becomes very fatigue resistant and the fatigue index (FI) decreases sharply. Thus, unoperated control EDL muscles have a FI of 0.83± 0.04 ($n = 11$) whereas following nerve crush at 3 days, the FI drops to 0.38± 0.14 ($n = 5$). However, treatment with leupeptin significantly improves the FI to 0.73 ± 0.10 ($n = 5$), which is similar to that observed in control muscles.

Thus, treatment with leupeptin prevents the reduction in muscle function that otherwise occurs as a consequence of nerve injury, possibly by inhibition of calpains.

Li L *et al.* (1998). *J Comp Neurol* **396**, 158–168.

Lowrie MB *et al.* (1987). *Brain Res* **428**, 91–101.

Wang KKW (2000). *Trends Neurosci* **23**, 20–26.

All procedures accord with current UK legislation.

C35

Age-related impairment in LTP in rat dentate gyrus is associated with an upregulation of interleukin-1β-induced cell signalling

Frank O. Maher and Marina A. Lynch

Trinity College Institute of Neuroscience, Department of Physiology, Trinity College, Dublin 2, Ireland

Hippocampal-dependent cognitive function has been shown to decline with age and this is paralleled by an age-related decrease in long-term potentiation (LTP). Upregulation of pro-inflammatory signalling pathways is believed to contribute to this decline. We tested this hypothesis by analysing interleukin-1β-induced signalling events in aged animals which did and did not sustain LTP in perforant path granule cell synapses.

Aged (22–24 months; $n = 14$) and young (2–3 months; $n = 6$) male Wistar rats were anaesthetized by intraperitoneal injection of urethane (1.5 g kg^{-1}) and assessed for their ability to sustain LTP following perforant path stimulation (3 trains of stimuli; 250 Hz for 200 msec; 30sec interval). The animals were killed 45 min after tetanic stimulation by decapitation and the hippocampus removed and stored for later analysis of IL-1β, interleukin-4 (IL-4), brain-derived neurotrophic factor (BDNF) and insulin-like growth factor-1 (IGF-1) by ELISA, and phosphorylation of c-Jun N-terminal kinase (JNK), extracellular signal regulated kinase (ERK) and c-Jun by gel-electrophoresis and Western immunoblotting.

Statistical analysis was carried out by one-way ANOVA in conjunction with a *post hoc* Student-Newmann-Keuls test. Data are shown as means ± S.E.M. and considered significant when $P < 0.05$ ($^*P < 0.05$; $^{**}P < 0.01$; $^{***}P < 0.001$).

Parameter	Young	Aged (LTP)	Aged (No LTP)
LTP 40-45min (epsp slope %)	115.5±4.16 ***	147.6±9.8 ***	93.7±6.2
IL-1β (pg/mg protein)	377.9±48.26	729.3±49.8 ***	904.8±29.93 ***/※
p-JNK (arbitrary units)	4421±218.1	4454±157.5	6719±1010 **
c-Jun (arbitrary units)	821.7±6.943	1245±43.24	1478±142.7 **
IL-4 (pg/mg protein)	44.76±9.4	26.27±7.2	12.52±2.6 **
BDNF (pg/mg protein)	93.71±28.3	41.95±6.5 *	37.16±4.7 *
IGF-1 (pg/mg protein)	86.06±12.9	72.19±17.54 *	28.5±7.4 *
p-ERK (arbitrary units)	7092±524.5	7414±457.1 *	5522±563.3 *

LTP was sustained in all young rats; seven aged rats sustained LTP and seven did not. Percentage changes in EPSP slope in the last 5 min of the experiment are shown in the table. We show evidence that age-related impairment in LTP is associated with an upregulation in IL-1β concentration and the activity of its downstream signalling components, JNK and c-Jun, as previously shown (Vereker *et al.* 2000). These changes were not seen in aged animals that sustained LTP. The age-related impairment in LTP was also associated with a significant decline in the concentration of BDNF, IL-4 and IGF-1 concentrations and activation of ERK. Thus, attenuation of survival signaling is also likely to contribute to the observed age-related impairment of LTP.

Vereker E *et al.* (2000). *J. Neurosci.* **20**, 6811–6819.

All procedures accord with current National and local guidelines.

C36

Irradiation upregulates IL-1β-induced cell signalling in hippocampus: protective effect of eicosapentaneoic acid

A.M. Lynch, M. Moore, S. Craig, P.E. Lonergan and Marina A. Lynch

Institute of Neuroscience, Department of Physiology, Trinity College, Dublin 2, Ireland

Radiotherapy treatment has been shown to result in deficits in hippocampal-dependent cognitive function. We set out to assess the possibility that whole body gamma-irradiation increases hippocampal IL-1β concentration and investigate the downstream consequences.

Male Wistar rats were housed in four groups ($n = 6$ per group); two groups were fed on laboratory chow (control diet) and two groups were fed on chow supplemented with 250 mg eicosepentaneoic acid (EPA; 1% diet) for 4 weeks. Next, two groups (control and 1% diet) were exposed to whole body irradiation (10 Gy at a rate of 10 Gy min^{-1}) and the two remaining groups were sham-irradiated. All groups were monitored for 4 days, anaesthetized by intraperitoneal injection of urethane (1.5g kg^{-1}) and assessed for their ability to sustain long term potentiation (LTP) in perforant path granule cell synapses. At the end of the electrophysiological recording, rats were killed by decapitation and the hippocampus was removed for analyses (Lonergan *et al.* 2002). Statistical analysis was assessed by a one-way ANOVA followed by a *post hoc* Student-Newmann-Keuls test. Data are represented by means ± S.E.M. and considered significant when $P < 0.05$ ($^*P < 0.05$; $^{**}P < 0.01$; $^{***}P < 0.001$).

Parameter	Sham-Irradiated		γ-irradiated	
	Con	1%	Con	1%
LTP 40-5min (epsp slope %)	134.1± 3.6	122.7± 3.4	96.8± 12.5 *	117.9± 1.4
IL-1β (pg/ml)	655.3± 42.8	764.7± 35.2	1007± 105.8 *	713.5± 47.0
IL-1RI (arbitrary units)	56.9± 1.8	54.7± 3.9	72.2± 6.5 *	57.1± 9.2
IL-1RAcP (arbitrary units)	50.1± 1.1	58.5± 3.7	76.7± 4.9 ***	57.4± 1.9
p-JNK (arbitrary units)	42.9± 2.8	48.2± 2.8	63.2± 4.7 ***	48.7± 4.1
p-ERK (arbitrary units)	46.1± 8.8	57.0± 4.5	26.4± 2.8 *	54.5± 8.2
Cytochrome c (arbitrary units)	37.9± 3.8	33.2± 2.4	63.8± 9.7 *	42.5± 6.2
PARP (arbitrary units)	53.1± 4.1	52.3± 2.8	32.3± 2.4 ***	56.5± 5.4
TUNEL (% pos cells)	19.6± 2.9	16.3± 2.2	36.9± 3.2 **	29.3± 2.2
IL-10 (pg/ml)	63.3± 3.7	36.2± 8.3	25.9± 7.5	141.5± 8.4 **

Table 1: Parameters assessed from sham and irradiated rats which received either control or 1% diet. See below for abbreviations.

We present evidence which reveals that irradiation leads to cell death in the hippocampus, and as a consequence, LTP is markedly impaired. The irradiation-induced increase in IL-1β concentration in hippocampus is accompanied by increased expression of IL-1 type I receptor and IL-1 accessory protein. These changes are coupled with increased activation of c-Jun N-terminal protein kinase (p-JNK), decreased activation of extracellular signal regulated kinase (p-ERK), and with evidence of cell death; namely parallel increases in cytochrome c translocation, poly(ADP-ribose)polymerase (PARP) cleavage and Tdt-mediated dUTP nick-end labelling (TUNEL) staining. Significantly, the irradiation-induced changes in hippocampus are abrogated by treatment of rats with EPA. When the irradiation-induced cell death was prevented by EPA, LTP was sustained in a manner similar to that in the control group.

Lonergan PE *et al.* (2002). *J Biol Chem* **277**, 20804–20811.

This work was supported by the Health Research Board (Ireland)

All procedures accord with current National and local guidelines.

C37

Intracortical and thalamic connections in layers Va and b of the rat cortex

N.F. Wright, L. Carroll and K. Fox

Cardiff School of Biosciences, Cardiff University, Cardiff CF10 3US, UK

The topographical representation of the large facial whiskers in the somatosensory cortex is known as the 'barrel cortex' where each whisker is represented as a single barrel in layer IV of the cortical column. Stimulation of a single whisker produces the greatest response in the anatomically corresponding barrel and forms the centre receptive field (CRF). However, other surround whiskers also generate lesser responses in the same barrel and form the surround receptive field (SRF). A central question for understanding the functional organisation of the cortex is to discover what pathways are responsible for the CRF and SRF. In this study we examined this question for layer V cells.

These experiments were conducted on six urethane (1.5g (kg body weight)$^{-1}$, I.P.) anaesthetised rats of both sexes, and after each experiment the rat was killed humanely. These experiments used a combination of global inhibition of cortical activity by the $GABA_A$ agonist muscimol in conjunction with local reactivation by iontophoresis of the $GABA_A$ antagonist bicuculline (Fox *et al.* 2003). This technique permits the receptive field properties to be studied in the absence of intracortical activity. Diffusion of muscimol through the cortical column was monitored by the loss of stimulated whisker activity at increasing depths after the application of 500 μM muscimol to the surface of the cortex. The loss of activity in the cortical column was ensured to a depth of 1500 μm before bicuculline was iontophoretically released from a multibarrelled recording electrode to locally reactivate neurones.

Preliminary data show reactivated Va cells have extensive SRFs in the absence of intracortical activity, whereas reactivated layer Vb cells show only CRFs in the absence of intracortical activity. If the data are reanalysed on the basis of response latency, then it is apparent that the short latency cells receive single whisker inputs, while long latency cells receive multiple whisker inputs. These data suggest that short latency response cells, mainly located in layer Vb receive their SRF input intracortically, while longer latency response cells receive their SRF input from a subcortical source or perhaps another cortical area (S II).

Fox K *et al.* (2003). *J Neuroscience* (in the Press).

This work was funded by the MRC.

All procedures accord with current UK legislation.

C39

Signalling pathways for experience-dependent CRE-mediated gene expression in mouse barrel cortex

John A. Curry, John R.S. Porter and Kevin Fox

Biosi 2, School of Biosciences, Cardiff University, Museum Avenue, Cardiff CF10 3US, UK

Phosphorylation of CREB (CRE binding protein) at its serine 133 residue has been implicated in plasticity in the hippocampus and neocortex. CREB binds to a DNA region known as CRE (cAMP response element) to initiate gene expression. CRE-mediated gene expression increases in the barrel cortex following single whisker experience (Barth *et al.* 2000). In this study we tested the hypothesis that the MEK and PKA pathways were responsible for activating experience-dependent gene expression in barrel cortex by using specific inhibitors in transgenic mice containing a CRE reporter gene (CRE-LacZ).

CRE–Lac Z mice were anaesthetized with avertin (I.P. injection 0.1 ml, 5 g), and implanted with osmotic mini-pumps (Azlet), which had a canula attached that was placed several millimetres anterior to the barrel cortex in the left cerebral hemisphere. We used three groups, a control group ($n = 4$) which had pumps filled with saline (0.9 %), a MEK inhibitor (UO126) group (50 mM) (Promega) ($n = 4$), and a cAMP inhibitor (Rp-8-ClcAMPS) group (5 mM) (Biomol) ($n = 2$). All but the D1 whiskers on both sides of the face were removed, and the mice were placed in an environmentally enriched cage for 16 h, after which they were anaesthetized with isoflurane (5 %), and killed by decapitation. The brains were then removed and reacted to quantify β-galactosidase activity using X-gal. Quantification was carried out by sectioning horizontally, mounting and counterstaining with propidium iodide. Numerical analysis was carried out by counting the number of X-Gal positive cells within the D1 barrel, and was expressed as a percentage of the total number of cells within the barrel. At least two observers counted the cells, and the results were averaged. An ANOVA statistical test was carried out between the MEK inhibited and the control group of hemispheres. The same was carried out for the deprived C1 and E1 barrels.

There was significant CRE-Lac Z expression in the D1 barrel of both hemispheres in the control animals. In animals receiving inhibitors, there was a significant reduction in CRE-LacZ expression in the left hemisphere treated with UO126 though not complete abolition ($P < 0.005$). This implies that MEK is an important factor for experience-dependent CRE-mediated gene expression in the barrel cortex. Similarly in brains treated with the cAMP inhibitor, CRE-mediated gene expression was reduced but not abolished. These preliminary observations also implicate adenylate cyclase and PKA in CRE-mediated gene expression.

Barth *et al.* (2000). *J Neurosci* **20**, 4206–4216.

All procedures accord with current UK legislation.

PC10

Neuronal damage in organotypic hippocampal slice cultures from rat: from epileptiform activity-induced damage to excitotoxicity

Paul J.E. Smith and Ruth M. Empson

School of Biological Sciences, Royal Holloway, University of London, Egham, Surrey TW20 0EX, UK

In experimental animal models and in human surgical tissue from intractable epileptics, there is often sclerosis of the hippocampus. Here we demonstrate in a slice model, a semiquantitative method to compare the damage induced by three agents reported to induce seizure-like activity: bicuculline (Bic), a $GABA_A$ receptor antagonist; 3-nitropropionic acid (3-NPA), an inhibitor of succinate dehydrogenase; and kainic acid (KA), a known excitotoxin.

Hippocampal slices (250 μm) from humanely killed neonate Wistar rats (P7) were maintained *in vitro* for 12–14 days before use (Stoppini *et al.* 1991). Slices were exposed to Bic (10 μM), 3-NPA (100 μM), or KA (25 μM) for 4 h, followed by 15 h recovery. A dual-stain fluorescent assay was used to assess viable (calcein-AM, 4 μM) and damaged cells (propidium iodide, 20 μM). Confocal images were collected (Bio-Rad) from four randomly selected areas within hippocampal subregions CA1 and CA3, using a $\times 60$ water-immersion objective. Fluorescence area was determined using Simple-PCI (C-Imaging). All values are means ± S.E.M. from slices from four separate animals.

All three agents caused varying degrees of cell death with clear differences between hippocampal subregions. Slices exposed to Bic and 3-NPA showed similar patterns of damage: CA1 was 5–6 times more vulnerable than CA3. However, 3-NPA caused approximately twice the damage in both subregions compared with Bic (543.6 ± 148.8 and 108.6 ± 37.2 μm^2 with Bic, compared with 1218.5 ± 370.4 and 201.4 ± 89.7 μm^2 with 3-NPA in CA1 and CA3, respectively). In contrast, KA caused the most extensive neuronal damage in both CA1 and CA3 (2644.7 ± 154.6 and 2560.9 ± 191.6 μm^2, respectively, $P < 0.001$, $n = 4$, ANOVA). Regions from control slices showed minimal cell damage (47.5 ± 15.2 and 42.4 ± 13.2 μm^2 for CA1 and CA3).

Neither Bic nor 3-NPA altered the area of total calcein staining compared to controls. However, an increase in the number of isolated sites where neurones were no longer present (or 'holes'), was seen in Bic-treated (2.0 ± 0.7 and 0.8 ± 0.6 for CA1 and CA3, respectively) and 3-NPA-treated slices (4.6 ± 1.1 and 1.3 ± 0.9 for CA1 and CA3) when compared with controls (0.3 ± 0.3 and 0.2 ± 0.1 for CA1 and CA3; $P < 0.01$, $n = 4$, ANOVA). KA, whilst further increasing the 'holes' (9.2 ± 2.2 and 6.7 ± 1.4 for CA1 and CA3), also resulted in increased calcein-stained area from swollen but surviving neurones ($P < 0.05$, $n = 4$, ANOVA).

This technique has identified a spectrum of hippocampal damage, ranging from mild to severe, at an early time point following treatment, with subregion differences. Our approach provides ways of assessing subtle neuronal damage that may be relevant to the development of intractable epilepsy, associated with hippocampal sclerosis.

Stoppini L *et al.* (1991). *J Neurosci Meth* **37**, 173–182.

We acknowledge the support of Action Research.

All procedures accord with current UK legislation.

PC11

Naturally secreted and synthetic β-amyloid-induced block of LTP in the rat hippocampus: mediation via activation of the mGluR5 receptor

Qinwen Wang*, Dominic M. Walsh†, Dennis J. Selkoe†, Michael J. Rowan‡ and Roger Anwyl*

Department of Physiology 1 and ‡Pharmacology and Therapeutics, Trinity College, Dublin 2, Ireland, and †Department of Neurology, Harvard Medical School and Center for Neurologic Disease, Brigham and Women's Hospital, Boston, MA 022115, USA

The action of naturally secreted cell-derived Alzheimer's disease β-amyloid (Aβ) and synthetic Ab1–42 were investigated on the induction of LTP in the rat medial perforant path to dentate granule cell synapse *in vitro*.

The animals were humanely killed. Both cell-derived and synthetic Aβ strongly inhibited high frequency stimulation (HFS)-induced LTP. In control slices in physiological media, HFS induced LTP measuring 151 ± 6 % (mean ± S.E.M.) at 60 min post-HFS ($P < 0.005$, $n = 8$, Student's unpaired t test). In the presence of synthetic Aβ (200 nM), LTP induction measured 115 ± 7 % ($P < 0.005$, $n = 8$). In the presence of conditioned medium containing cell-derived Aβ collected from 7PA2 cells secreting nanomolar concentrations of soluble Aβ, LTP induction measured 110 ± 7 %, $n = 6$ $P < 0.005$, compared with 188 ± 10 %, $n = 6$, in control medium collected from non-transfected CHO cells. Baseline transmission was not altered by synthetic or cell-derived Aβ. The involvement of metabotropic glutamate receptors (mGluRs) in the Aβ-mediated block of LTP induction was investigated by applying Aβ in the presence of the group I/II mGluR antagonist LY341495 and the mGluR5 antagonist MPEP. Both antagonists prevented the inhibition of LTP induction by synthetic Aβ, LTP measuring 147 ± 3 % and 141 ± 9 %, respectively, $n = 5$, $P < 0.005$. In addition, the group I mGluR agonist DHPG lowered the threshold concentration for the inhibitory action of Aβ. Thus 100 nM synthetic Aβ was found to inhibit LTP induction in the presence of the selective group I agonist DHPG (20 μM) (129 ± 4 %, $P < 0.005$, $n = 5$), but not in control media (146 ± 10 %, $n = 5$).

We would like to thank the Wellcome Trust for financial support

All procedures accord with current National and local guidelines.

PC12

An NMDAR-independent LTP mediated by group II metabotropic glutamate receptors and p42/44 MAP kinase in the rat dentate gyrus *in vitro*

Jianqun Wu*, Michael J. Rowan† and Roger Anwyl*

Department of Physiology and †Pharmacology and Therapeutics, Trinity College, Dublin 2, Ireland

The induction of long-term potentiation (LTP) under conditions of blockade of the *N*-methyl-D-aspartate receptor (NMDAR) was studied in the medial perforant path to granule cell synapse in the rat dentate gyrus.

Animals were killed humanely. A single brief high frequency stimulation (HFS) induced a small amplitude NMDAR-independent potentiation (115 ± 6 %, $n = 11$, $P < 0.01$, mean ± S.E.M., Student's unpaired t test) at 10 min post-HFS in 100 μM AP5. Further HFS applied at 10 min intervals increased the amplitude of LTP induction such that after the 3rd HFS, NMDAR-independent LTP was induced measuring 139 ± 7 % ($n = 11$, $P < 0.01$) at 30 min post-HFS. The NMDAR-independent LTP was most likely to be mediated by activation of group II mGluR. Thus the NMDAR-independent LTP induced by three spaced HFS was inhibited by the group I/II antagonist LY341495 (5 μM), with HFS-inducing long-term depression (LTD) measuring 38 ± 6 % ($n = 6$, $P < 0.01$), and by the group II mGluR antagonist EGLU (100 μM), with HFS-inducing LTD measuring 32 ± 8 % ($n = 5$, $P < 0.01$). The mGluR5 antagonist MPEP did not inhibit the LTP induction, which measured 131 ± 6 % ($n = 5$). Perfusion of the group II mGluR agonist DCG-IV induced NMDAR-independent LTP measuring 126 ± 9 % ($n = 6$, $P < 0.01$) in media containing the NMDAR antagonist AP5, although LTD was induced in control media. The NMDAR-independent LTP induced by three spaced HFS was mediated via activation of p42/44 MAP kinase as it was blocked by the selective inhibitor PD98059, with LTD being induced by HFS measuring 37 ± 5 % ($n = 8$, $P < 0.01$).

We would like to thank the Wellcome Trust for financial support.

All procedures accord with current National and local guidelines.

PC13

Signalling mechanism of $GABA_B$ receptor-mediated inhibition of GABA release onto mouse cerebellar Purkinje cells: potential involvement of a direct effect on the release machinery

Gary J. Stephens

Department of Pharmacology, University College London, Gower Street, London WC1E 6BT, UK

At many central synapses, exocytotic release of GABA is modulated by the activation of presynaptic $GABA_B$ receptors. In contrast to detailed structural knowledge, $GABA_B$ receptor signalling mechanisms remain somewhat unresolved (Misgeld *et al.* 1995); furthermore, a more novel mechanism whereby G protein-coupled receptors (GPCRs) may directly couple to the exocytotic machinery has been shown in lamprey motoneurons (Blackmer *et al.* 2001). Here, I examined the major signalling pathways proposed to couple to $GABA_B$ receptor activation in mammalian central neurons by investigating the effects of $GABA_B$ receptor activation on inhibitory GABAergic transmission onto Purkinje cells.

Inhibitory postsynaptic currents (IPSCs) and miniature IPSCs (mIPSCs) were recorded using whole-cell patch-clamp recordings in parasagittal cerebellar slices, obtained from humanely killed 3- to 5-week-old mice. Data are presented as means ± S.E.M. (n), where n is the number of cells.

The $GABA_B$ receptor agonists baclofen and CGP 44533 (both 25 μM) caused a clear, reversible reduction in mean IPSC frequency. In subsequent experiments, the effects of a number of agents on this baclofen-induced inhibition were determined (Fig. 1). In all of these experiments, no clear effects were seen on mean IPSC (or mIPSC) amplitude, consistent with a presynaptic site of action. Baclofen inhibition was blocked by the $GABA_B$ antagonist CGP 55845 (5 μM). Baclofen effects were also occluded by *N*-ethylmaleimide (NEM; 50 μM), an alkylating agent which uncouples $G_{\alpha o}/G_{\alpha i}$ subunits. Baclofen inhibition was unaffected by the general voltage-dependent Ca^{2+} channel blocker Cd^{2+} (50 μM) and the general K^+ blocker Ba^{2+} (100 μM). Also, baclofen still produced a robust inhibition of mIPSCs isolated by tetrodotoxin (TTX, 1 μM). Under these conditions, the adenylate cyclase inhibitor SQ 22536 (100 μM) also did not prevent baclofen inhibition. Finally, the secretagogue ruthenium red (10 μM) was used to directly stimulate the synaptic release machinery (see Bardo *et al.* 2002). Importantly, baclofen was able

to inhibit GABA release under these conditions, in which other downstream mechanisms were bypassed. However, baclofen inhibition was attenuated in comparison to controls ($P < 0.01$), which may be consistent with a convergent site of action for ruthenium red and baclofen.

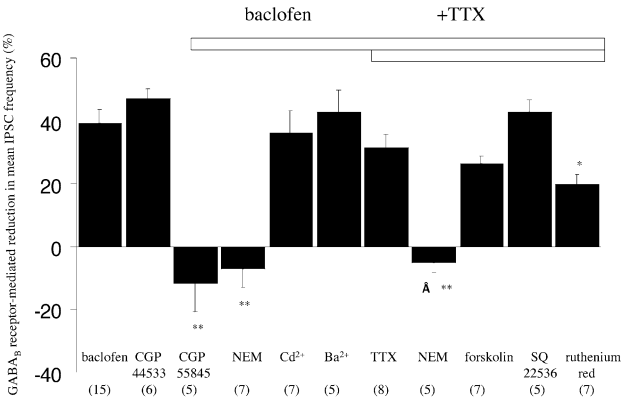

Figure 1. Effect of agents on baclofen-induced inhibition of mean (
m)IPSC frequency; $*P < 0.01$, $**P < 0.001$ Student's unpaired *t* test.

This study provides evidence that $GABA_B$ receptor-mediated inhibition of GABA release onto Purkinje cells involves $G_{\alpha o}/G_{\alpha i}$ (or their liberated $G_{\beta\gamma}$) subunits and that action occurs downstream of any effects on major ion conductances or adenylate cyclase. The action of baclofen in the presence of ruthenium red is consistent with a signalling pathway involving a direct interaction with the synaptic machinery in this pathway.

Bardo S *et al.* (2002). *Br J Pharmacol* **137**, 529–537.
Blackmer T *et al.* (2001). *Science* **292**, 293–297.
Misgeld U *et al.* (1995). *Prog Neurobiol* **46**, 423–462.

This work was supported by The Wellcome Trust.

All procedures accord with current UK legislation.

PC14

Characterisation of Ca^{2+} mobilisation by P2 receptor agonists in rat dorsal root ganglion sensory neurons

A.J. Currie, E.G. Rowan and C. Kennedy

Department of Physiology and Pharmacology, University of Strathclyde, 27 Taylor Sreet, Glasgow G4 ONR, UK

We have previously shown that ATP and α,β-meATP evoke rapid inward currents via $P2X_3$ receptors in dissociated neurones of the rat DRG (Robertson *et al.* 1996; Rae *et al.* 1998). The aim of this study was to characterise the rise in cytoplasmic $[Ca^{2+}]_i$ elicited by ATP and α,β-meATP in these neurones using the fluorescent dyes fura-2 and fluo-4. The responses were also compared with those evoked by capsaicin.

Sprague-Dawley rats of either sex (3–7 days) were humanely killed. DRG from all spinal levels were dissected aseptically and dissociated enzymatically. Cells were perfused at 8 ml min^{-1} with a Hepes-based buffer. Drugs were applied in the perfusate for 20 s. Only cells that responded to KCl (50 mM) were included in the analysis.

Initially, we used fura-2 to quantify the agonist-induced rise in cytoplasmic $[Ca^{2+}]$ in single cells. KCl (50 mM) evoked a reversible rise with a peak of 207 ± 11 nM (mean ± S.E.M.) ($n = 108$). An increase was also evoked by ATP (100 μM) in 29/44 cells (peak = 75 ± 9 nM), by capsaicin (10 μM) in 16/36 cells (peak = 143 ± 26 nM) and by α,β-meATP (30 μM) in 11/28 cells (peak = 45 ± 6 nM).

Subsequently, we used fluo-4 to measure the responsiveness of populations of cells. Here, the mean peak increase in fluorescence evoked by KCl (50 mM) was 2.0 ± 0.1 $\Delta F/F_0$ ($n = 174$). An increase in fluorescence was evoked by ATP (100 μM) in 95/174 cells (peak = 1.4 ± 0.1 $\Delta F/F_0$), by capsaicin (10 μM) in 156/174 cells (peak = 2.5 ± 0.2 $\Delta F/F_0$) and by α,β-meATP (30 μM) in 102/174 cells (peak = 0.9 ± 0.1 $\Delta F/F_0$).

Subsequently, we determined the role of extracellular $[Ca^{2+}]$ in these responses. Under zero $[Ca^{2+}]_o$ conditions all KCl- ($n = 154$) and α,β-meATP- ($n = 49$) evoked changes were abolished. In contrast, an increase in fluorescence was seen in 23% of ATP-sensitive cells and 30% of capsaicin-sensitive cells. For both drugs, the peak rise was smaller than in the presence of $[Ca^{2+}]_o$ (0.7 ± 0.1 and 0.18 ± 0.08$\Delta F/F_0$ respectively).

Thus, these results show that the depolarising currents induced by ATP, α,β-meATP and capsaicin are associated with a rise in intracellular $[Ca^{2+}]$. For α,β-meATP the rise is entirely dependent upon Ca^{2+} influx, whereas ATP and capsaicin induce both Ca^{2+} influx and release.

Rae MG *et al.* (1998). *British J Pharmacol* **124**, 176–180.
Robertson SJ *et al.* (1996). *British J Pharmacol* **118**, 951–956.

A.J.C. holds an MRC sudentship

All procedures accord with current UK legislation.

PC15

Distribution of markers for glucose sensing neurones in the rat brainstem

R.H. Balfour and Stefan Trapp

Royal Free and University College Medical School, Department of Physiology, Rowland Hill Street, London NW3 2PF, UK

The lower brainstem has been implicated in the monitoring of brain glucose levels, but the mechanisms employed are unclear. In order to investigate whether brainstem glucose sensing involves similar mechanisms to that of pancreatic β-cells, we have tested for the presence of glucokinase and the glucose transporter Glut-2 in the rat brainstem. Additionally, hexokinase I was used as a control.

Sprague Dawley rats (150 g) were anaesthetised (Sagatal; 60 mg kg^{-1}, I.P.) and transcardially perfused with 4% paraformaldehyde. The brain was removed and 40 μm coronal brainstem sections cut using a vibratome. Sections were incubated with polyclonal antibodies against glucokinase (1:50; Santa Cruz Biotechnologies), hexokinase I (1:50; Santa Cruz), or Glut-2 (1:500, 1:100; Biogenesis), then with biotin-labelled secondary antibodies and visualized by horseradish peroxidase staining (Ni-enhanced DAB). For mRNA isolation, rats were decapitated under anaesthesia, the brainstem removed, sliced, further dissected and mRNA isolated using a kit (Quiagen).

Strong glucokinase immunoreactivity was observed in ependymocytes lining the central canal and the fourth ventricle. Slightly weaker signals were obtained from large cell bodies in the hypoglossal and dorsal vagal nucleus and from small cells in the nucleus of the solitary tract (NTS) and the area postrema. Discrete staining was also found in the ventral medulla within the

raphe pallidus, and the pyramidal tract. Hexokinase I immunoreactivity was seen in hypoglossal and dorsal vagal neurones, within the nucleus of the solitary tract, and in the area postrema. Ependymocytes did not show hexokinase I immunoreactivity. Furthermore, staining was observed within the reticular nucleus of the ventrolateral brainstem.

Glut-2 immunoreactive cells included ependymocytes lining both the central canal and fourth ventricle. In contrast to the results for glucokinase, the cilia of these cells stained for Glut-2. Additionally, hypoglossal, NTS, and dorsal vagal neurones exhibited Glut-2 immunoreactivity. Within the ventral part of the medulla, raphe pallidus and pyramidal tract cells were immunoreactive.

RT-PCR confirmed that mRNA encoding glucokinase, Glut2 and hexokinase is present in the central, lateral and ventrolateral brainstem.

In summary, our results suggest that proteins involved in glucose sensing are present in discrete areas of the lower brainstem. Immunoreactivity for Glut-2 and glucokinase is largely overlapping Surprisingly, also hexokinase I immunoreactivity shows a similar distribution. It remains to be verified if all cells expressing glucokinase and Glut-2 actually act as central glucose sensors and if glucokinase and hexokinase I are co-expressed in some cells.

This work was supported by an MRC Career Development Award to ST.

All procedures accord with current UK legislation.

PC17

The aminoguanidine carboxylate BVT.12777 activates K_{ATP} channels in hypothalamic glucose-responsive neurones

S. Mirshamsi, D. Spanswick and M.L.J. Ashford

*Department of Pharmacology & Neuroscience, University of Dundee, Ninewells Hospital & Medical School, Dundee DD1 9SY, Scotland and *Department of Biological Sciences, University of Warwick, Coventry CV4 7AL, UK*

Leptin and insulin modulate the excitability of hypothalamic glucose responsive (GR) neurones by activation of K_{ATP} channels (Spanswick *et al.* 1997, 2000). Activation of K_{ATP} channels is potentially important in mediating the physiological effects of these hormones. Thus, we have examined the effects of a novel weight-reducing agent, BVT.12777, on GR neurone K_{ATP} channels.

Sprague-Dawley rats were humanely killed by cervical dislocation prior to decapitation. Whole-cell current-clamp recordings from arcuate nucleus (ARC) neurones in coronal hypothalamic slices, and single channel recordings from acutely isolated ARC neurones were made, as previously described (Spanswick *et al.* 1997). For cell-attached recordings, electrodes contained a high (140 mM) K^+ solution and neurones were bathed in 135 Na^+-containing saline. Inside-out recordings were made in symmetrical K^+ at −40 mV. Mean channel activity was determined as N_fP_o (where N_f is the number of functional channels and P_o the open state probability) over a 120 s period. Means ± S.E.M. are given. Statistical analysis used Student's unpaired *t* test.

Bath application of BVT.12777 (200 μM) caused hyperpolarisation, cessation of firing and reduced input resistance of GR neurones recorded in slices ($n = 5$), effects reversed on bath application of tolbutamide (200 μM, $n = 3$). Cell-attached recordings from acutely dispersed neurones showed that BVT.12777 (100 μM), in the recording electrode or bath applied, increased K^+ channel activity in 58 % of patches ($n = 18/31$). Mean N_fP_o, 1–2 min following patch formation was 0.09 ± 0.03 and was 0.47 ± 0.12 after 5–15 min ($n = 10$; $P < 0.01$). BVT.12777-induced channel activity was inhibited by tolbutamide (200 μM) from a mean value of 0.43 ± 0.05 to 0.25 ± 0.03 ($n = 4$; $P < 0.05$). However, in contrast to leptin and insulin, BVT.12777-induced K_{ATP} channel activity was not reversed by the PI 3-kinase inhibitor, wortmannin (10 nM, $n = 4$). Inside-out patches displayed K^+ channel activity which was inhibited by 3 mM MgATP ($n = 6$) and consistent with the large conductance K_{ATP} channels. BVT.12777 (100 μM), in the presence of MgATP, increased mean channel activity from 0.09 ± 0.03 to 0.47 ± 0.03 ($n = 6$; $P < 0.05$) in inside-out patches.

Thus, BVT.12777 activates the large conductance K_{ATP} channel in hypothalamic GR neurones but, unlike leptin and insulin, this action is not driven by a membrane receptor-mediated process nor mediated by PI 3-kinase.

Spanswick D *et al.* (1997). *Nature* **390**, 521–525.

Spanswick D *et al.* (2000). *Nature Neurosci* **3**, 757–758.

This work was supported by Biovitrum and the Wellcome Trust.

All procedures accord with current UK legislation.

PC18

K_{ATP} currents in the vagal complex of the medulla

A.M. Kruse Hansen*, P. Wahl* and S. Trapp†

**Novo Nordisk A/S, Research and Development, Maaloev, Denmark and †Royal Free and University College Medical School, Department of Physiology, Rowland Hill Street, London NW3 2PF, UK*

The dorsal vagal nucleus (DVN), the nucleus of the solitary tract (NTS) and the area postrema (AP) are essential for diverse autonomic functions, including the processing of visceral satiety signals. We have analysed the distribution of K_{ATP} currents within these areas as a marker for intrinsic metabolic sensitivity of these neurones. Furthermore, we have correlated the presence of K_{ATP} channels with other electrical properties of vagal neurones.

Brainstem slices (200 μm) were obtained from 18- to 25-day-old Sprague-Dawley rats after terminal anaesthesia (Sagatal; 60 mg kg^{-1}; I.P.) and transcardial perfusion with Na^+-free solution. After recovery at 34 °C for 30 min, slices were kept in ACSF at room temperature. Whole cell recordings were established with borosilicate capillaries (2–4 MΩ) filled with (mM): 120 potassium gluconate, 1 NaCl, 1 $MgCl_2$, 1 $CaCl_2$, 10 Hepes, 10 EGTA, pH 7.2 and K_2ATP.

Thirty-three per cent of DVN ($n = 54$), 54 % of NTS ($n = 35$) and all AP neurones ($n = 8$) possessed functional K_{ATP} channels, as examined with K_{ATP} channel openers (diazoxide (200 μM), NNC 55–9216 (100 μM)), or by tolbutamide (500 μM) block of spontaneous, or cyanide-induced (1 mM), K_{ATP} currents. These were observed in 46 % of all recordings independent of the pipette ATP concentration (0−5 mM). However, cells expressing K_{ATP} channels opened these spontaneously in 11 of 16 recordings with ATP-free pipette solution, in 2 of 19 with 1 mM ATP, and in no recordings with higher ATP concentrations.

NNC55-9216 is a specific opener for K_{ATP} channels containing SUR1, but not SUR2A or SUR2B (Dabrowski *et al.* 2002). K_{ATP} currents that were sensitive to diazoxide, but not to NNC 55-9216 were not observed. This suggests that most brainstem K_{ATP} channels are of the SUR1 type.

The majority of DVN and NTS neurones have slowly inactivating K^+ currents. Seventy-five per cent of DVN and 56 % of NTS

neurones without these currents also lacked K_{ATP} currents. In contrast, H-type inward currents were only observed in a small subpopulation of cells (10 out of 97), but 9 of these showed K_{ATP} currents. T-type Ca^{2+} currents were observed in 5 cells; 3 of these had K_{ATP} currents.

Whilst K_{ATP} channels are abundant in these regions, only 8 of 123 neurones tested opened K_{ATP} channels in response to short term hypoglycaemia.

In summary, K_{ATP} channels are abundant in parasympathetic neurones, but probably less so in efferent than in afferent neurones. Their presence alone is not indicative of glucose sensitivity. The results also suggest that the intracellular ATP concentration of these cells remains mainly governed by cell metabolism in whole cell recordings.

Dabrowski M *et al.* (2002). *Diabetes* **51**, 1896–1906.

This work was supported by an MRC Career Development Award to S.T. and by Novo Nordisk A/S.

All procedures accord with current UK legislation.

PC19

Electrophysiological characterisation of the substantia gelatinosa of adult rat spinal cord

R. Nicholson*†, D. Spanswick† and K. Lee†

** Pfizer Global Research and Development, Cambridge University Forvie Site, Cambridge CB2 2QB and † Department of Biological Sciences, University of Warwick, Coventry CV4 7AL, UK*

The substantia gelatinosa (SG) is a vital integrative centre for sensory information arriving from peripheral nerves. Despite receiving both noxious and innocuous input, the identity of distinct cell types within the SG remains to be fully established (Gobel 1978; Light *et al.* 1979). In order to further the understanding of information processing within the adult rat SG, we have attempted to define neuronal cell types based upon their characteristic electrophysiological properties.

Intrinsic cell properties were examined using parasagittal spinal cord slices (150–300 μm) prepared from terminally anaesthetised male Wistar rats (240–400g). Slices were superfused (2.5 ml min^{-1}, 35 °C) with artificial cerebrospinal fluid containing (mM): 125 NaCl, 25 $NaHCO_3$, 10 glucose, 2.5 KCl, 1.25 NaH_2PO_4, 2 $CaCl_2$, 1 $MgCl_2$, and bubbled with 95 % O_2–5 % CO_2. Whole-cell patch-clamp recordings were made from visually identified SG neurons, using electrodes filled with (mM): 120 potassium gluconate, 10 NaCl, 2 $MgCl_2$, 0.5 K_2EGTA, 10 Hepes, 4 Na_2ATP, and 0.3 Na_2GTP, pH 7.2. Data are presented as mean ± S.E.M.; statistical significance was confirmed with Student's unpaired *t* test.

Under current-clamp recording conditions, current–voltage relationships obtained by the injection of negative and positive current steps revealed differential expression of active conductances in SG neurons in the presence of 1 μM TTX. From these data we classified neurons into clusters based upon the expression patterns of these conductances. Cluster 1 was characterised by a hyperpolarisation-activated cation conductance (I_h, $n = 69$), sensitive to 1 mM Cs^+ ($n = 8$). A further 49 Cluster 1 neurons expressed a T-type Ca^{2+} conductance, sensitive to 100 μM Ni^+ ($n = 4$). Cluster 2 neurons expressed anomalous inwardly rectifying K^+ conductances (I_{an}, $n = 49$), sensitive to 100 μM Ba^{2+} ($n = 10$); and Cluster 3 neurons expressed both I_h and I_{an} ($n = 25$). Cluster 4 neurons were characterised by the presence of an A-type K^+ conductance ($n = 5$), sensitive to 2 mM 4-aminopyridine ($n = 3$). Cluster 5 neurons expressed a T-type conductance ($n = 9$) and Cluster 6 expressed both I_{an} and an A-type K^+ conductance ($n = 21$). These conductances were absent in all Cluster 7 neurons ($n = 48$). Significant cluster-specific variations were observed throughout cell properties, including resting membrane potential (Cluster 3: −59 ± 1.2 mV, Cluster 4:−67 ± 5 mV ($P < 0.01$)), firing threshold (Cluster 5: −35 ± 2.8 mV, Cluster 6: −24 ± 1.9 mV ($P < 0.01$)) and input resistance (Cluster 1: 247 ± 17.7 MΩ, Cluster 2: 432 ± 26.6 MΩ ($P < 0.01$)).

In conclusion, we have demonstrated the presence of electrophysiological phenotypes within the SG. How they differentially integrate afferent information remains to be defined.

Gobel S, (1978). *J Comp Neurol* **180**, 395–414.

Light AR *et al.* (1979). *J Comp Neurol* **186**, 151–172.

All procedures accord with current UK legislation.

PC20

Amyloid β protein regulates K^+ channel expression in cultured rat neurones

N.J. Webster*, L.D. Plant†, J.P. Boyle*, C. Peers* and H.A. Pearson†

** Schools of Medicine and † Biomedical Sciences, University of Leeds, Leeds LS2 9JT, UK*

The A-type K^+ current (I_{KA}) is functionally increased in cerebellar granule neurones (CGN) by exogenous treatment with 10–100 nM amyloid β protein 1–40 (Aβ; Ramsden *et al.* 2001), the Alzheimer's disease-related peptide that is constitutively cleaved from its precursor protein by β- and γ-secretases. In agreement with this, inhibitors of β- and γ-secretase reduce endogenous Aβ levels in CGN and significantly diminish I_{KA}. This reduction in current is rescued by co-application of 1 nM Aβ (Plant *et al.* 2002). Here we use Western blotting techniques to investigate the effects of exogenous Aβ treatment and γ-secretase inhibition on the expression levels of Kv4.2 and Kv4.3, the K^+ channel α-subunits thought to mediate I_{KA}.

CGN were isolated and cultured from humanely killed 6-day-old neonatal rats as previously described (Ramsden *et al.* 2001). Whole cell lysates were prepared after 7 days and Western blot analysis of 10 % SDS–PAGE gels was performed using polyclonal antibodies raised against Kv4.2 and Kv4.3 α-subunits. Quantification of the bands was performed by laser scanning densitometry and data are given as means ± S.E.M.

Following 24 h treatment with 100 nM Aβ there was a significant increase in the expression of Kv4.2 and Kv4.3 by 49 ± 11 % ($P < 0.02$, Student's paired *t* test, $n = 4$) and 45 ± 20 % ($P < 0.05$, $n = 5$), respectively. Kv4.2 expression showed a significant increase of 45 ± 11 % ($P < 0.05$, $n = 4$) as rapidly as 2 h after Aβ treatment but no significant effects were seen following 48 h treatment (−24 ± 19 %, $n = 5$). In contrast to its effects on I_{KA} (Plant *et al.* 2002), the γ-secretase inhibitor 2-naphthoyl-VF-CHO (γ-IV, 10 μM) had no significant effect on the expression of Kv4.2 (protein expression was 96 ± 11 % of control levels, $n = 5$). Furthermore, at a concentration of Aβ (1 nM) that can negate the reduction in current observed following treatment with γ-IV (Plant *et al.* 2002), there was no significant effect of Aβ on the protein expression levels of Kv4.2 channels (protein expression was 100 ± 24 % of controls in the presence of γ-IV and 1 nM Aβ, $n = 5$). These results were confirmed qualitatively by immunofluorescent labelling of permeabilised cells with an antiKv4.2 polyclonal antibody.

Thus, exogenous Aβ causes a rapid transient increase in Kv4.2

expression that mirrors changes seen in I_{KA}. Block of endogenous Aβ production reduces I_{KA} but has no effect on Kv4.2 protein expression, suggesting an effect that may be mediated by changes in trafficking of Kv subunits. Our data provide further support for a physiological role for Aβ in regulating K^+ channel function in the central nervous system.

Plant LD *et al.* (2002). *J Physiol* **544.P**, 9*P*.
Ramsden M *et al.* (2001). *J Neurochem* **79**, 699–712.

This work was supported by The Wellcome Trust.

All procedures accord with current UK legislation.

PC21

5-Hydroxytryptamine-mediated recovery from the block of LTP induction by acute stress in the rat hippocampus *in vivo*

B.K. Ryan*, R. Anwyl† and M.J. Rowan*

**Department of Pharmacology and Therapeutics, Trinity College, Dublin 2, Ireland and †Department of Physiology, Trinity College, Dublin 2, Ireland*

The ability to induce long-term potentiation (LTP) in the intact hippocampus has been shown to be greatly impaired following exposure to an inescapable elevated platform stress (Xu *et al.* 1997). Recently a role for the serotonergic system in the mediation/modulation of the effects of stress on LTP has been suggested (Shakesby *et al.* 2002). In the present study we investigated the ability of serotonergic agents to overcome the block of LTP by stress.

Male Wistar rats (240–360 g) had electrodes implanted into the stratum radiatum of the CA1 region of the dorsal hippocampus under urethane anaesthesia (1.5 g kg^{-1}, I.P.). Test field EPSP amplitude was 50 % of the maximum and was increased to 75 % maximum during high frequency stimulation (HFS). The Department of Health, Republic of Ireland licenced the experimental protocol including the humane method of killing. HFS (10 trains of 20 stimuli at 200 Hz) induced stable LTP of the field EPSP in non-stressed rats ($n = 5$; 136 ± 6 % of baseline 60 min after HFS; $P < 0.001$, compared with pre-HFS baseline: mean ± S.E.M., Student's paired t test). In contrast, in animals that were immediately anaesthetised after being exposed to the elevated platform stress for 30 min, HFS failed to induce LTP ($n = 5$; 102 ± 5 %; $P > 0.05$). (±)Fenfluramine (5 mg kg^{-1}, I.P.), a 5-HT releaser and 5-HT uptake inhibitor, was found to reverse the stress-induced block of LTP ($n = 7$; 140 ± 9 %; $P < 0.005$). The effect of (±)fenfluramine was prevented by pre-treatment with (±)tianeptine (2 mg kg^{-1}, I.P.), an agent that promotes 5-HT uptake ($n = 7$; 109 ± 10 %; $P > 0.1$). This provides evidence that the recovery of LTP was due to the ability of (±)fenfluramine to raise brain 5-HT levels. Consistent with this, the 5-HT_2 receptor antagonist cinanserin (30 mg kg^{-1}, I.P.) also prevented the effect of (±)fenfluramine ($n = 5$; 107 ± 13 %; $P > 0.5$). Further evidence for the involvement of 5-HT_2 receptors was the recovery of LTP in stressed rats treated with the 5-$HT_{2B/2C}$ receptor agonist mCPP (1-(3-chlorophenyl)piperazine, 10 mg kg^{-1}, I.P.) ($n = 5$; 154 ± 15 %; $P < 0.01$).

It is concluded that raising brain 5-HT levels can overcome the effects of inescapable stress on synaptic plasticity by activation of 5-HT_2 receptors.

Shakesby AC *et al.* (2002). *J Neurosci* **22**, 3638 −44.
Xu L *et al.* (1997). *Nature* **387**, 497–500.

This work was supported by Science Foundation Ireland and the Irish Higher Education Authority.

All procedures accord with current National guidelines.

PC22

Role of FMRFamide in the reproduction of *Octopus vulgaris*: molecular analysis and effect on visual input

Carlo Di Cristo and Anna Di Cosmo

Department of Biological and Environmental Sciences, University of Sannio, Benevento, Italy

As a part of continuous research on the neurobiology of the cephalopods in general, and the neuroendocrine control of reproduction in *Octopus vulgaris* in particular (Di Cosmo & Di Cristo, 1998), the presence, the molecular analysis and the effect of FMRFamide on the screening-pigment migration in the visual system have been analysed.

FMRFamide presence was revealed by using a monoclonal antibody against this tetrapeptide. Immunoreactive fibres are present in the outer plexiform layer of the retina as well as in the plexiform zone of the deep retina (n of experiments =10; all the animals were humanely killed) (Young, 1971). These fibres presumably come from optic and olfactory lobes. We isolated an incomplete *Octopus* FMRFamide cDNA by using 3′ and 5′ rapid amplification cDNA ends method (3′,5′ RACE). The cDNA encodes for a peptide precursor containing several FMRFamide-related peptides (FaRPs) showing a high degree of identity with the FaRPs encoded in the precursor of *Sepia officinalis*, except for the presence of a FLRPamide peptide which is known to be present only in cnidarians. Finally, stimulation of isolated retina demonstrated the effect of this tetrapeptide, coupled with dopamine (Gleadall *et al.* 1993), is the induction of an extreme adaptation of the retina to the light condition. This situation *de facto* inhibits sexual maturation. Our results on the negative modulation of FMRFamide confirms the suggested hypothesis that this peptide play an inhibitory role on the activity of optic gland.

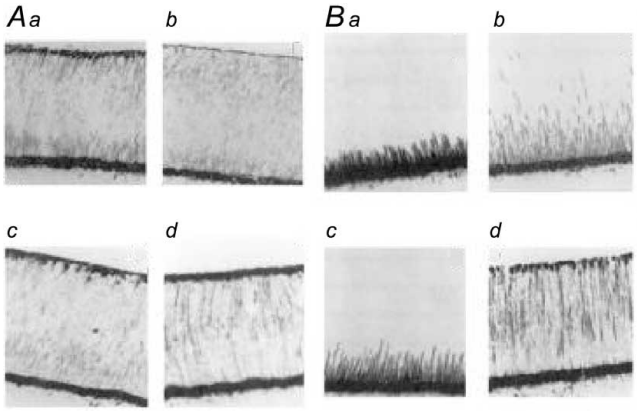

Figure 1. I, effect of dopamine and FMRFamide on the screening pigmant migration on light-adapted retinae of *Octopus vulgaris*. *A*, control preparations incubated in oxygenated filtered sea water. Pigment is locate in the tips of photoreceptors. *B,* dopamine incubation causes a quick proximal displacement of pigment granules and the apical regions of photoreceptors are almost clear of pigment. *C,* Incubation with FMRFamide does not produce any apparent effect of pigment distribution compared to the control. *D,* incubation with dopamine and FMRFamide induces a block of the pigment in the apical tips of

photoreceptors. II, effect of dopamine and FMRFamide on the screening pigmant migration on dark-adapted retinae of *Octopus vulgaris*. *A*, control preparations incubated in oxygenated filtered sea water. Pigment is locate in the basal zone of the photoreceptors. *B*, dopamine incubation causes a slow distaldisplacement of pigment granules. *C*, Incubation with FMRFamide does not produce any apparent effect of pigment distribution compared to the control. *D*, Incubation with dopamine and FMRFamide induces a fast migration of the screening-pigment toward the apical tips of photoreceptors.

Di Cosmo A & Di Cristo C (1998). *J Comp Neurol* **398**, 1–12.

Gleadall, I. G *et al.* (1993). *J Exp Biol* **185**, 1–16.

Young, J. Z. (1971). *The Anatomy of Nervous System of* Octopus vulgaris. Clarendon, Oxford.

All procedures accord with current National guidelines.

PC23

Modulation of paired pulse inhibition/facilitation by stimulation of $\alpha4\beta2$ nicotinic receptors in dentate gyrus of anaesthetized rats

Lucy Ayre, Yun Wang, Elaine Shanks and David Lodge

Lilly Research Centre, Eli Lilly & Co. Ltd Erl Wood Manor, Sunninghill Road, Windlesham, Surrey GU20 6PH, UK

Paired pulse stimulation of perforant pathway evokes a triphasic (early paired pulse inhibition (ePPI), paired pulse facilitation (PPF) and late PPI (lPPI) response in the dentate gyrus (DG). The ePPI is modulated by activation of $GABA_B$ receptors (Canning & Leung, 2000). We have revalidated this modulation and then investigated whether nicotinic receptors are also involved in this paired pulse paradigm.

Male Sprague-Dawley (SD) rats (body weight 250–350 g) were anaesthetized with urethane (1.25 mg kg^{-1}, I.P.). All animals were humanely killed at the end of the experiments. The lateral tail vein was cannulated for drug administration, and the femoral artery was cannulated for blood pressure monitoring. Body temperature was maintained at 37 ± 10 °C by a homeothermic heat pad. Field excitatory postsynaptic potentials (fEPSPs) and population spikes (PS) were evoked in the DG by bipolar stimulation of the perforant pathway and recorded using a glass electrode (filled with 2 % Pontamine sky blue in 2 M NaCl with an *in vitro* impedance of 2.5–3.0 mΩ). PS amplitude was used as a measure of DG granule cell excitability. Experiments were carried out at 70 % of the maximum PS amplitude. PPI/PPF was evoked with an inter-pulse interval (IPI) between 20 and 1000 ms.

Baclofen (0.03–3 mg kg^{-1}, I.V. $n = 2$–6), a $GABA_B$ receptor-selective agonist, dose dependently inhibited both ePPI and PPF but not lPPI. This inhibition was prevented by CGP35348 (200 mg kg^{-1}, I.V. $n = 6$), a selective $GABA_B$ antagonist. TC2559 (2 mg kg^{-1}, I.V. $n = 6$), an $\alpha4\beta2$-selective partial agonist, reversibly, repeatedly and differentially affected ePPI, lPPI and PPF in DG. The ePPI was significantly ($P < 0.01$, Student's paired *t* test) inhibited by TC2559, at an IPI of 25 ms, from a control of 57.5 ± 4.4 % (mean ± S.E.M.) to 36.4 ± 4.8 %. In contrast, the PPF and lPPI were all significantly ($P < 0.05$) enhanced, from 4.0 ± 6.3 % to 69.7 ± 17.2 % (IPI of 90 ms) for PPF and from 16.6 ± 2.8 % to 42.5 ± 4.6 % (IPI of 500 ms) for lPPI, respectively. DHβE (1 mg kg^{-1}, I.V. $n = 6$), an $\alpha4\beta2$-preferring antagonist, fully reversed the TC2559 effect on PPF and lPPI, but only partially on ePPI.

In conclusion, stimulation of $\alpha4\beta2$ nicotinic receptors can modulate the DG paired pulse index. This modulation may contribute to nicotinic facilitation of the short-term neuronal plasticity in DG.

Canning KJ & Leung LS (2000). *Brain Res* **863**, 271–275.

All procedures accord with current UK legislation.